# Fatigue of the Cement/Bone Interface: The Surface Texture of Bone and Loosening

**D. Arola, K. A. Stoffel, D. T. Yang**

Department of Mechanical Engineering, University of Maryland Baltimore County, 1000 Hilltop Circle, Baltimore, Maryland 21250

*Received 7 January 2005; revised 3 March 2005; accepted 25 April 2005*
*Published online 3 August 2005 in Wiley InterScience (www.interscience.wiley.com). DOI: 10.1002/jbm.b.30364*

**Abstract: Loosening is recognized as one of the primary sources of total hip replacement (THR) failure. In this study the influence of the bone surface texture on loosening of the cement/bone interface was studied. Model cemented hip replacements were prepared and subjected to cyclic loads that induced pure shear fatigue of the cement/bone interface. The femoral canals were textured with the use of specific cutting tools to achieve a desired surface topography. Loosening of the implant with cyclic loading was characterized in terms of the initial migration (Region I), steady-state loosening (Region II), and unstable loosening (Region III). Results from the experiments showed that the initial migration and rate of steady-state loosening were dependent upon the bone surface topography. The apparent fatigue strength ranged from 0.8 to 5.1 MPa, and denotes the cyclic shear stress required for loosening of 1 mm within 10 million cycles. Regardless of the bone surface topography the ratio of apparent fatigue strength and ultimate shear strength of the interfaces was approximately 0.24. In general, the apparent fatigue strength increased proportional to the average surface roughness of the femoral canal and the corresponding volume available for cement interdigitation. In addition, there was a strong correlation between the normalized initial migration and the apparent fatigue strength (i.e., specimens with the highest initial migration exhibited the lowest fatigue strength).** © 2005 Wiley Periodicals, Inc. J Biomed Mater Res Part B: Appl Biomater 76B: 287–297, 2006

**Keywords: bone cement; fatigue; loosening; implant**

## INTRODUCTION

The long-term success of cemented total hip replacements (THRs) is often limited by loosening of the femoral component.[1–5] Loosening is considered a complicated function of both mechanical and biological factors.[6] Despite widespread recognition of the problem, the specific mechanisms responsible for initiation and progression loosening are not completely understood.

The majority of research on the femoral side of cemented hip replacements has focused on improving the cement/prosthesis interface. Clinical evidence suggests that failures, and the incidence of loosening along the cement/bone interface, are prevalent.[7,8] Improvements in the cement/prosthesis interface have reportedly increased normal stresses across the cement/bone interface.[7,9,10] Certainly, failure at the cement/bone interface is an issue, regardless of the condition of the cement/prosthesis interface. Thus, the interfacial strength has become increasingly important. Push-out and shear tests are regularly used to assess the shear strength of the cement/bone interface,[11–14] and results have been reported between[11] 1 MPa and 63 MPa.[13] The large range in reported strength is believed to be attributable to variations in cement penetration along the interface.[15–19]

The strengths of the cement/prosthesis and cement/bone interfaces are influenced by the surface texture of both the prosthetic device and bone.[19–24] The surface texture controls interdigitation of the cement and the extent of mechanical interlock. Mann et al.[19] evaluated mechanical properties of the cement/bone interface under tension and the effects of bone density and cement/bone interdigitation. Increasing the volume of cement in trabecular bone was recommended for maximizing the interface strength and reducing the incidence of interface failure. Aggressive endosteal core reaming during canal preparation generally reduces the amount of endosteal bone available for cement/bone interdigitation. Thus, mechanical interlock between cement and trabecular bone may be limited, especially for revisions or if the patient has suffered from osteoporosis.

A total hip replacement will be subjected to a combination of monotonic and cyclic loads. Consequently, fatigue is a critical concern and the fatigue properties of cortical and

*Correspondence to:* D. Arola (e-mail: darola@umbc.edu)
Contract grant sponsor: Maryland Chapter of the Arthritis Foundation

cancellous bone have received considerable attention.[25,26] A similar degree of effort has been placed on evaluating the response of bone cement to cyclic loading.[27–29] Yet fatigue failure of the cement/bone interface has not been examined in detail. Kim, Miller, and Mann[30,31] recently examined the cement/bone interface using both shear and tensile fatigue. Sliding at the interface and within the interdigitated region promoted permanent deformation in both modes of loading and was characterized as creep deformation. Although it is highly significant, the influence of surgical preparation and corresponding bone surface texture on the fatigue response was not considered. At present the influence of surface texture and the volume of cement interdigitation on the fatigue strength of the bone/cement interface remains unknown.

In this study the fatigue properties of the cement/bone interface were studied using model cemented total hip replacements. Loosening was quantified in terms of displacement that evolved between the cement and bone as a function of cyclic loading. The primary objective of the investigation was to examine the importance of bone surface texture on the incidence and progression of loosening in cemented total hip replacements.

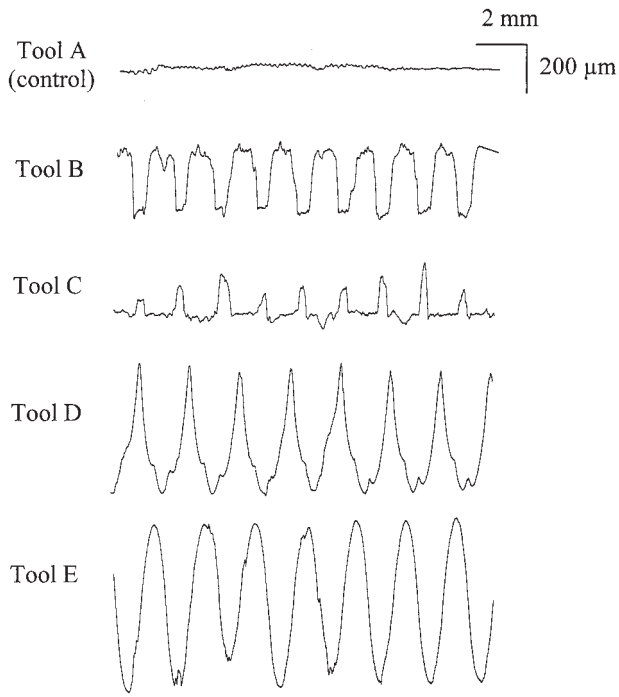


**Figure 1.** Surface profiles of the femoral canal resulting from use of the five different cutting tools. The profiles have been acquired parallel to the canal. Note the difference in vertical and horizontal scales.

## METHODS AND MATERIALS

Bovine rear femurs were obtained from a local slaughterhouse within 24 h of slaughter. Transverse sections were obtained from the middiaphysial region of the femurs with length of approximately 25 mm. More than 60 femurs were used to obtain 60 suitable sections with adequate wall thickness ($t \leq 5$ mm) and canal diameter ($d \leq 25$ mm). The femoral canal of each section was enlarged to approximately 30 mm, and then expanded to the final diameter of 31.7 mm with one of five different cutting tools. After preparation the canal wall was comprised of cortical bone only. One tool served as the control and was used to impart a canal texture similar to that resulting from use of an endosteal broach. Four additional tools were designed and developed to impart a specific canal surface texture. The surface texture of the canals was processed with the use of specific tools to enable an objective evaluation of the effects from surface topography of the bone on interdigitation and fatigue strength. All five of the tools exhibited a single cutting edge and were used in oscillating mode, which resulted in the primary lay along the circumferential direction. The bone was maintained throughout these procedures in a calcium-buffered saline solution[32] at room temperature. Surface profiles of the bone resulting from preparation were obtained parallel to the axis of the femoral canal. Representative profiles of the bone surfaces prepared with Tool A (control), and Tools B–E are shown in Figure 1.

Prior to cementing the femoral canal surface texture resulting from surface preparation was analyzed with a Hommel T8000 contact profilometer and a skid-type sensing probe with a 10-$\mu$m-diameter diamond stylus. Profiles were obtained parallel to the canal with the use of a traverse length of 15 mm and cutoff length of 2.5 mm. The average surface roughness ($R_a$) was calculated according to DIN 4762. Bearing height curves were constructed from surface profiles obtained from the femoral canals and used in estimating the core roughness ($R_k$), reduced peak height ($R_{pk}$), and reduced valley depth ($R_{vk}$) according to DIN 4776. The total volume available for cement interdigitation ($V_i$) within the bone topography was then estimated according to[33]

$$V_i = \frac{R_{pk}(M_{r1})}{200} + (R_{pk} + \frac{R_k}{2}) \cdot \frac{(M_{r2} - M_{r1})}{100} + (R_{pk} + R_k + \frac{R_{vk}}{2}) \cdot \frac{(100 - M_{r2}}{100} \quad (1)$$

where $M_{r1}$, $M_{r2}$ are the peak and valley material ratios for the surface profile and were available from the bearing height curves. The quantity $V_i$ defines the interdigitation volume over the profile traverse length per unit surface width. Surface profiles were also obtained of the bone and cement mantle surfaces after failure to distinguish changes in $V_i$ that occurred with fatigue and wear of the interface. Results of this aspect of the investigation are reported elsewhere.[34]

Model hip-replacement specimens were prepared from the sections of bone to simulate the femoral side (Figure 2). Each specimen consisted of a model implant cemented within a section of femur with canal that was prepared with a cutting tool (Figure 1). The model implants (also regarded as the stem) consisted of a section of Ti6Al4V rod with 100-mm length and 25.4-mm diameter. The stem and canal diameters

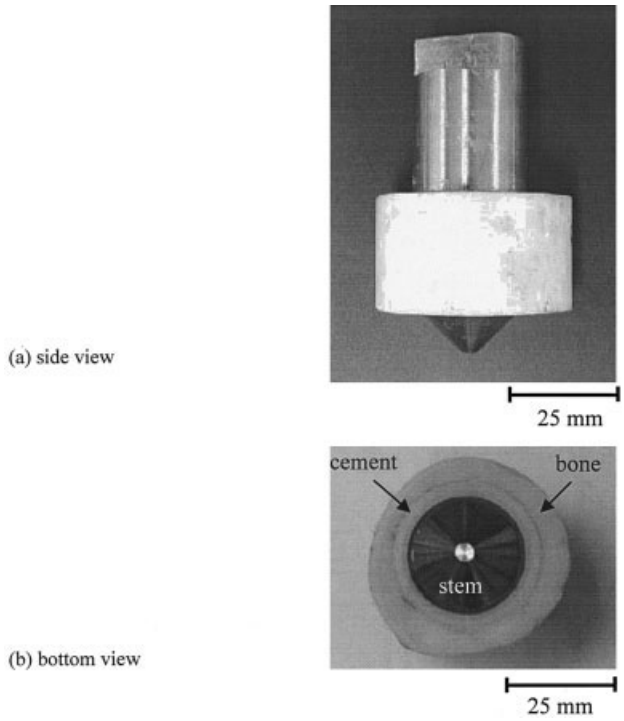


**Figure 2.** A completed model implant specimen. (a) Side view, (b) bottom view.

resulted in a cement mantle thickness of 3 mm, which is within the range suggested for minimizing failure of the cement.[35] One end of the stems was chamfered to simplify insertion within the canal during the cementing process. The surface of the stems was textured to minimize failure of the cement/stem interface. The bone cement* was mixed at room temperature in the recommended ratios and kneaded for 10 seconds to allow air bubbles to be released. An adequate volume of cement was placed within the prepared canal and the stem was then inserted with the use of a dedicated fixture that ensured that the stem and bone axes were concentric and parallel. Following insertion the cement mantle was pressurized to approximately 200 kPa, which is within the range reported in the open literature.[36] Pressurization was used to minimize cement voids and achieve complete interdigitation. After pressurizing for a period of 5 min the bone cement was allowed to fully cure at room temperature for no less than 30 min. Sacrificial specimens were also prepared with each of the cutting tools and sectioned (without fatigue loading) to confirm that interdigitation of the cement was fully achieved.

The fatigue life of the model implants was determined with the use of cyclic loads with magnitude defined with respect to the ultimate strength of the interface. Preliminary experiments were performed with selected specimens and the cyclic responses showed that the fatigue strength was largely dependent on the surface preparation. Although dependent on location, the primary stress at the cement/bone interface is shear. Therefore, a series of push-out tests were conducted with specimens representing each of the five surface preparations; the ultimate shear strength ($\tau_{ult}$) of the cement/bone interface correspond to the maximum push-out load. It is important to recognize that the ultimate shear strength is really an apparent measure that describes the nominal (average) shear stress along the interface. The maximum cyclic load was then chosen to achieve a maximum cyclic shear stress ($\tau_{max}$) corresponding to 30%, 40%, or 70% of $\tau_{ult}$. A haversine wave [Figure 3(a)] with a small reversal was chosen to simulate loads transmitted from the natural gait and was administered using load control actuation with frequency of 5 Hz. A minimum cyclic stress ($\tau_{min}$) of approximately 5% of the maximum stress was utilized to simulate forces of the abductor muscles during the swing phase of normal walking.[37,38] Note that the maximum load is defined such that the load and shear stress with largest magnitude are considered to be positive, as shown in Figure 3(b). The stress ratio resulting from the load (stress) cycle for all tests was $R = -0.05$, where $R = \tau_{min}/\tau_{max}$.

A total of 60 model implant specimens were prepared and tested, including 15 for push-out testing (five tools and three specimens each) and 45 for fatigue testing [five tools and three specimens each at three load levels (30%, 40%, and 70% $\tau_{ult}$)]. Both the push-out and fatigue tests were conducted with the use of either an INSTRON 1331A load frame or an MTS model 810 frame. The specimens were loaded within a specially designed fixture that enabled pure shear fatigue of the cement/bone interface [Figure 4(a)]. Hydration of the specimens was maintained in a calcium-buffered saline solution at room temperature. The instantaneous axial load and displacement were recorded with the use of the data-acquisition software of the respective universal test system every 2000 cycles at 100 Hz for 1 s; at this frequency five cycles of the cyclic response were recorded. A stroke limit was defined to discontinue cyclic loading when the axial displacement reached 1 mm. The maximum period of evaluation was 500,000 cycles, and was based upon the average number of steps a person takes a day over 6 months.[39]

Loosening was defined in terms of the stem displacement ($\delta$) that evolved with respect to the bone as illustrated in Figure 4(a). The instantaneous actuator displacement was examined over the fatigue life and used to quantify the evolution of loosening. The absolute displacement ($\delta_{abs}$) was

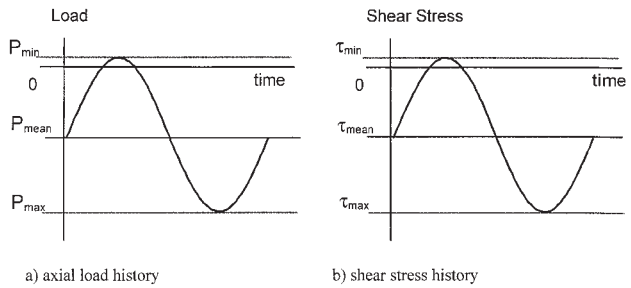


**Figure 3.** Definition of loads and corresponding shear stress resulting from fatigue loading. (a) Axial load history, (b) shear stress history.

*ENDURANCE™ styrene copolymer bone cement donated by DePuy®

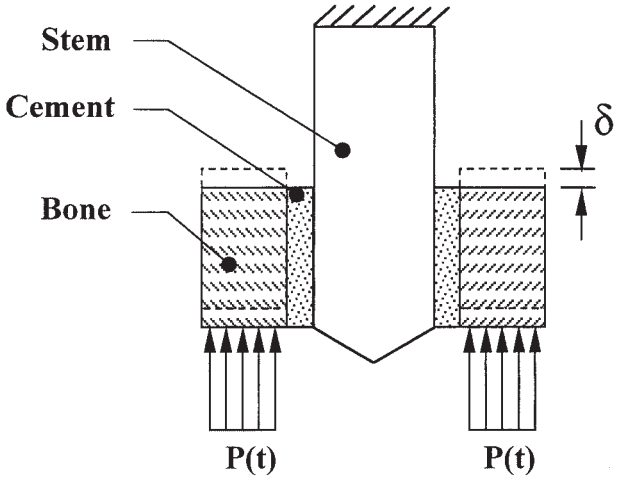


(a)

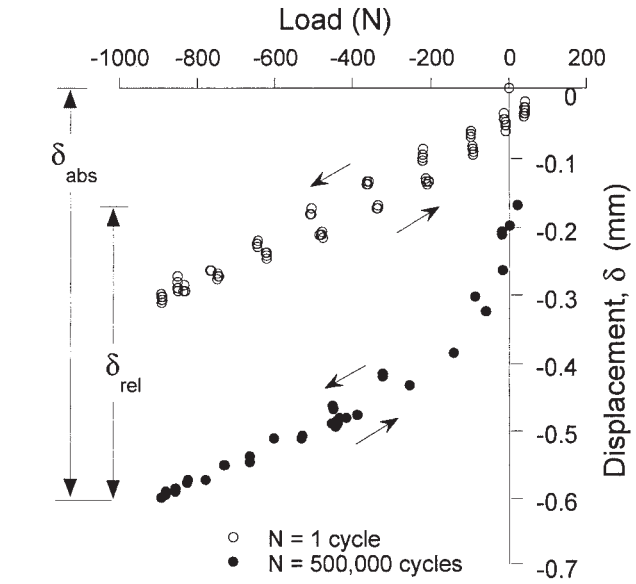


(b)

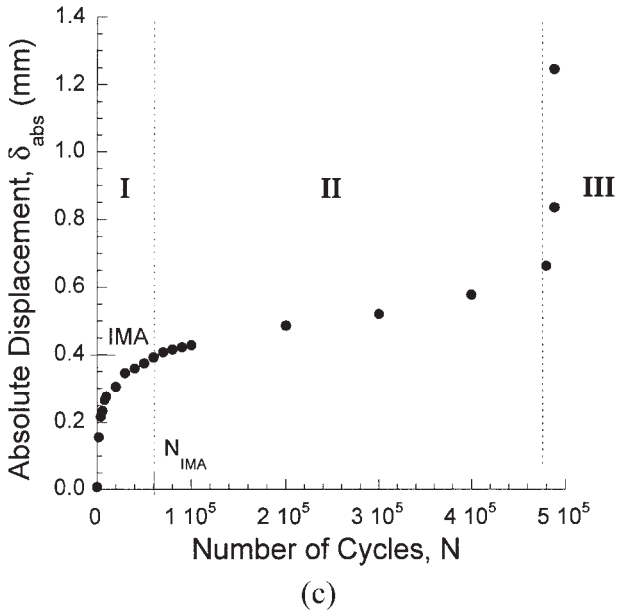


(c)

defined as the total stem displacement from the original position in the first cycle [Figure 4(b)]. Similarly, the relative displacement ($\delta_{rel}$) was defined as the stem displacement that evolved from the minimum to maximum load in one cycle. Both $\delta_{abs}$ and $\delta_{rel}$ were then examined over the total fatigue life (or 500,000 cycles, whichever was first). It was found that the $\delta_{abs}$ provided the most consistent measure of loosening and that the total migration to failure exhibited three distinct regions as evident in Figure 4(c); Regions I, II, and III were defined as the regions of initial migration, steady-state loosening, and unstable loosening, respectively. The initial migration and unstable loosening regions were identified from the displacement history according to the deviation in trend from the steady-state loosening response. An initial migration amplitude (IMA) and period of initial migration ($N_{IMA}$) were defined to describe the total stem displacement within Region I [Figure 4(c)]. Because the maximum stress used for fatigue loading was defined in terms of the push-out strength, the $\delta_{abs}$ was normalized by the maximum cyclic shear stress ($\delta_{abs}/\tau_{max}$). The normalized steady-state migration ($\hat{\delta}_{st}$) was modeled according to

$$\hat{\delta}_{st} = A' N^b, \quad N > N_{IMA} \quad [\mu m/MPa] \tag{2}$$

where $A'$ and $b$ are the normalized loosening coefficient and loosening exponent, respectively. Note that the quantity $b$ represents the (log–log) displacement rate of the power law relationship. Stress-life ($\tau$-$N$) diagrams were constructed from results of the fatigue tests in terms of the maximum cyclic shear stress and number of cycles to a critical displacement. An empirical relationship was developed for each of the $\tau$-$N$ diagrams according to

$$\tau_a = \alpha N^{\beta} \quad [MPa] \tag{3}$$

where $\alpha$ and $\beta$ are regarded as the fatigue-strength exponent and coefficient, respectively, and $N$ is the corresponding life. The quantities $\alpha$ and $\beta$ were determined for each bone surface preparation and were evaluated in terms of a critical displacement that defined failure of the cemented model implant; critical displacements of 0.2 and 1.0 mm were used. The apparent fatigue strength ($\tau_a$) of the interface was determined with the use of the models in terms of a specific number of cycles fatigue cycles ($N_f$) indicative of the life. Following failure (or after 500,000 cycles) the specimens were evaluated with the use of optical microscopy.

**Figure 4.** Details of the cyclic load, measures of displacement, and cyclic response used in characterizing loosening for the model implants. (a) Schematic diagram of the displacement and measure of loosening ($\delta$). (b) The displacement response for one load cycle. The arrows indicate the direction of loading and unloading. (c) The three distinct regions of loosening evident from a typical absolute displacement ($\delta_{abs}$) history. This response is for a 1-fluted specimen tested (Tool E) at 30% push-out strength.

**TABLE I. Properties of the Surfaces Resulting from Surface Preparation of the Femoral Canal and the Corresponding Shear Strength Estimated from Results of the Push-Out Tests**

| Surface/Tool | $R_a$ ($\mu$m) | $V_i$ ($\mu$m) | Shear Strength (MPa) |
|---|---|---|---|
| Tool A (Control) | 5 | 16 | 2.7 ± 0.6 |
| Tool B | 40 | 70 | 16.4 ± 2.4 |
| Tool C | 46 | 131 | 9.9 ± 1.2 |
| Tool D | 55 | 154 | 14.1 ± 1.2 |
| Tool E | 111 | 218 | 23.6 ± 2.4 |

## RESULTS

The average surface roughness ($R_a$) of the femoral canals, volume available for cement interdigitation ($V_i$) and shear strength ($\tau_{ult}$) of the cement/bone interfaces determined from results of the push-out tests are listed in Table I. Failure of all the model implants occurred at the cement/bone interface and there was no indication of loosening at the cement/prosthesis interface. The relationship between the $R_a$ and shear strength of the cement/bone interface is shown in Figure 5(a). As expected, the specimens with the lowest $R_a$ (i.e., the control surface) had the lowest $\tau_{ult}$, whereas specimens prepared with the highest $R_a$ (Tool E) had the highest $\tau_{ult}$. Although there was a general increase in strength with increase in $R_a$, results for the implants prepared with Tools B–D indicate that there are other important qualities of the surface topography besides the average roughness. As apparent from Figure 5(b), the shear strength appeared to increase linearly with $V_i$ as well, but exhibited lower correlation than with regards to $R_a$. None of the other surface roughness parameters exhibited strong correlation with the interface shear strength.

The shear strength of the cement/bone interfaces for each group of model implants was used in defining the maximum cyclic shear stress used for fatigue loading of the model implants. The fatigue response was quantified in terms of the $\delta_{abs}$ between the stem and bone (i.e., loosening). Regardless of the magnitude of cyclic loading, loosening and failure occurred along the cement/bone interface of all specimens. In general, the $\delta_{abs}$ history exhibited three characteristic regions of response corresponding to initial migration, steady-state loosening, and unstable loosening as shown in Figure 4(c). Typical responses for model implants prepared with Tool E and subjected to cyclic loading with 30%, 40%, and 70% $\tau_{ult}$ are shown in Figure 6(a–c), respectively. All specimens subjected to cyclic loads of 30% $\tau_{ult}$ exhibited Regions I–III. However, these three regions were less distinct in the responses that resulted from cyclic loading with 40% $\tau_{ult}$ [e.g., Figure 6(b)] and almost undetectable for 70% $\tau_{ult}$. For cyclic loading at 70% $\tau_{ult}$ the rate of loosening increased consistently from the onset of cyclic loading [Figure 6(c)] and the loosening history seldom exhibited the three-region response. As expected, the fatigue life decreased with increasing cyclic stress amplitude from for all five groups of specimens ($p < 0.01$). All specimens subjected to cyclic loading with maximum cyclic stress of 70% $\tau_{ult}$ reached $\delta_{abs}$ of 1 mm within 500,000 cycles. For cyclic loading with 40% $\tau_{ult}$ and 30% $\tau_{ult}$ all of the specimens displaced 1 mm within 500,000 cycles except for the specimens prepared with Tool A (control). Despite having the lowest $R_a$ and interface shear strength, the control specimens underwent $\delta_{abs}$ of less than 0.5 mm within 500,000 cycles.

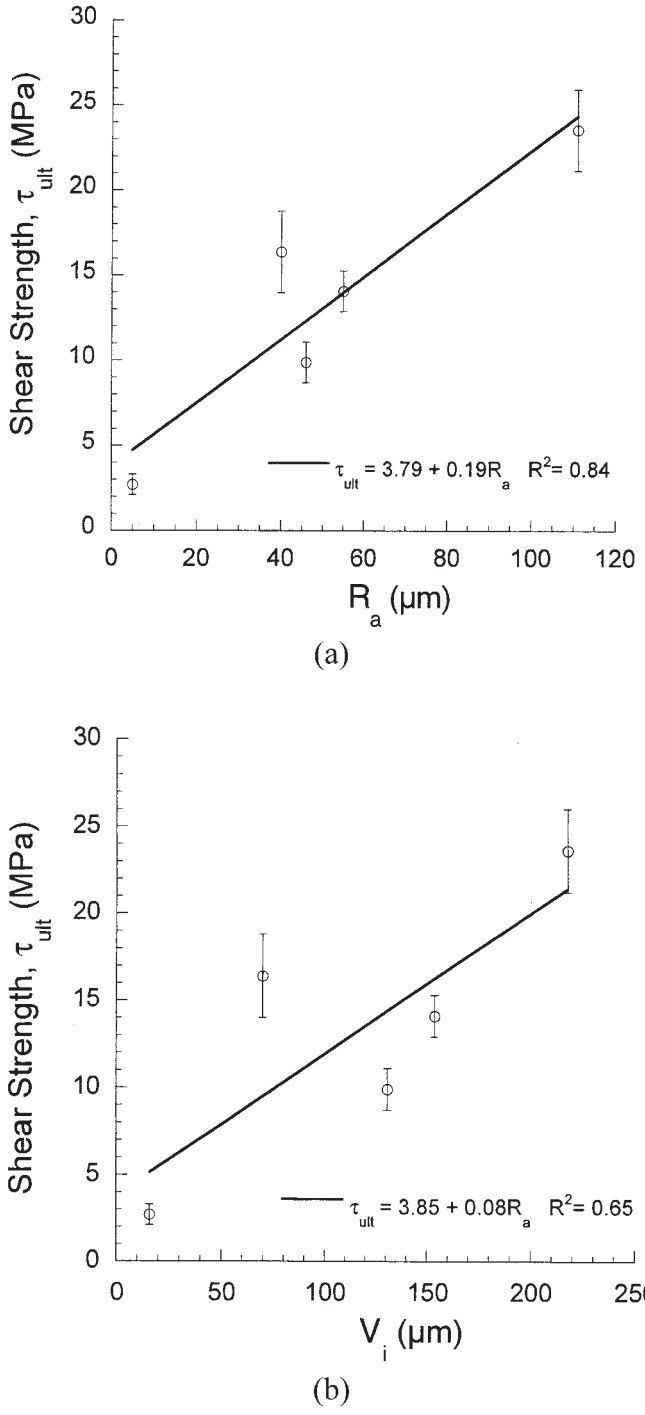


**Figure 5.** The influence of surface topography on the ultimate shear strength of the cement/bone interface. (a) Influence of average surface roughness ($R_a$), (b) influence of volume of interdigitation ($V_i$).

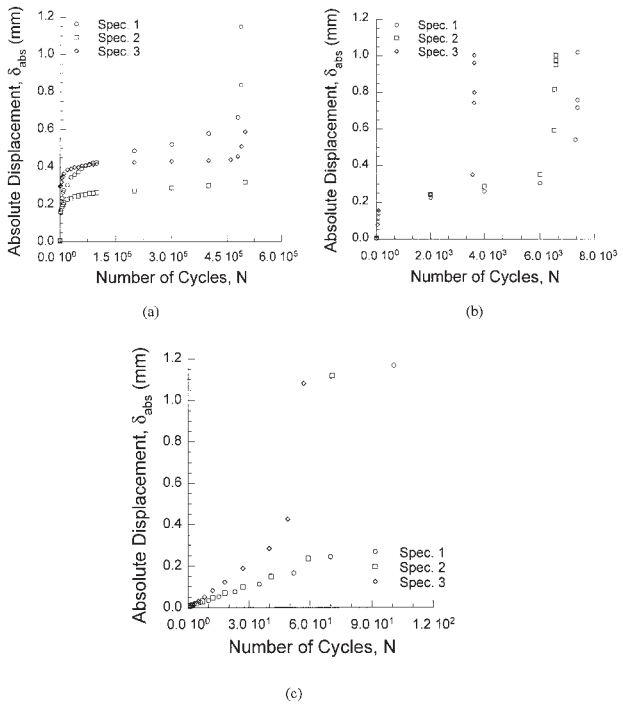


**Figure 6.** A comparison of the loosening history for the model implants prepared with highest surface roughness and volume of cement interdigitation (Tool E). Note the recession in Region I with increased magnitude of shear stress. (a) Cyclic load with 30% $\tau_{ult}$, (b) cyclic load with 40% $\tau_{ult}$, (c) cyclic load with 70% $\tau_{ult}$.

With the use of the absolute displacement history the three characteristic regions of loosening were quantified for all specimens. The IMA and period of initial migration ($N_{IMA}$) are listed for each group of model implants in Table II. The IMA resulting from fatigue loading with 70% $\tau_{ult}$ are not reported because a Region I response was not evident from the displacement history. According to a comparison of the responses for 30% and 40% $\tau_{ult}$ (Table II), the IMA decreased with an increase in the maximum cyclic shear stress ($\tau_{max}$) for all specimens. The results were significant ($p < 0.05$) for specimens prepared with Tool A and mildly significant for those specimens prepared with Tools D and E ($0.05 < p < 0.1$). With the exception of the control specimens, there was also a decrease in the $N_{IMA}$ with increase in $\tau_{max}$.

In addition to quantifying the Region I loosening behavior, the Region II responses were modeled in terms of a power-law response according to Equation (2). The normalized loosening coefficient ($A'$) and loosening exponent ($b$) for the model implants are listed in Table III. In general, the loosening exponent ($b$) increased with increasing $\tau_{max}$ from 30% to 70% $\tau_{ult}$, indicating that the rate of steady-state loosening increased with the maximum cyclic stress, as expected. The increase in $b$ with magnitude of cyclic shear stress was significant ($p < 0.01$) for all specimens except those prepared with Tool C. Interestingly, the model implants prepared with Tool C exhibited the highest loosening exponent ($b$) for cyclic loading, with 30% and 40% $\tau_{ult}$. The lowest average loosening exponent resulted from the control specimens, which also exhibited the highest loosening coefficient of all the model implant specimens.

The fatigue strength of the cement/bone interface was estimated using stress life ($\tau$-$N$) diagrams that were constructed with results of the fatigue tests and the push-out tests (where $N = 1$). The $\tau$-N diagram for a critical displacement of $\delta_{abs} = 1$ mm is shown in Figure 7(a). Each data point in this figure represents the average number of cycles required for $\delta_{abs} = 1$ mm; the error bars indicate the range in number of cycles to failure for three specimens. All of the implants reached $\delta_{abs}$ of 1 mm within 500,000 cycles, except for specimens prepared with Tool A (control), which did not fail from cyclic loading at either 30% or 40% $\tau_{ult}$. Stress-life diagrams were also prepared for $\delta_{abs} = 0.2$ mm [Figure 7(b)], which represents a more conservative definition of failure than that presented in Figure 7(a). The power-law exponent and coefficient as well as the degree of correlation of the models are listed in Table IV for each group of specimens. Overall, there was a high degree of correlation with $R^2 \geq 0.95$. The stress-life diagrams in Figure 7 represents the cyclic response limited to within the first 500,000 cycles, which is equivalent to approximately 6 months postoperation.[37] The high-cycle (long life) fatigue response ($N_f \geq 1 \times 10^6$) is of particular interest and can be estimated for the cemented implants with the use of the power-law models. The apparent fatigue strength ($\tau_a$) for each group of model implants was estimated for a life ($N_f$) of $10 \times 10^6$ cycles (Table IV) with the use of a critical displacement of 1.0 mm and the developed $\tau$-$N$ models. The control specimens exhibited the lowest fatigue strength of all the model implants, with $\tau_a \leq 1$ MPa. The ratio of the apparent fatigue strength to the ultimate tensile strength for specimens prepared with each of

**TABLE II. Average Initial Migration Amplitude (IMA) and Period of Initial Migration ($N_{IMA}$) for the Model Implant Specimens.**

| | 30% $\tau_{ult}$ | | 40% $\tau_{ult}$ | |
|---|---|---|---|---|
| Surface/Tool | IMA (mm) | $N_{IMA}$ (cycles) | IMA (mm) | $N_{IMA}$ (cycles) |
| Tool A | 0.36 ± 0.05 | 27E3 ± 11E3 | 0.18 ± 0.01 | 47E3 ± 11E3 |
| Tool B | 0.31 ± 0.03 | 19E3 ± 1E3 | 0.29 ± 0.04 | 2E3 ± 2E3 |
| Tool C | 0.25 ± 0.10 | 27E3 ± 11E3 | 0.24 ± 0.02 | 15E3 ± 5E3 |
| Tool D | 0.31 ± 0.10 | 37E3 ± 15E3 | 0.19 ± 0.03 | 2E3 ± 2E3 |
| Tool E | 0.35 ± 0.09 | 60E3 ± 1E3 | 0.26 ± 0.01 | 2E3 ± 1E3 |

**TABLE III. Steady-State Loosening Parameters for the Region II Responses**

| | 30% $\tau_{ult}$ | | 40% $\tau_{ult}$ | | 70% $\tau_{ult}$ | |
|---|---|---|---|---|---|---|
| Surface/Tool | $A'$ ($\mu$m/MPa) | $b$ | $A'$ ($\mu$m/MPa) | $b$ | $A'$ ($\mu$m/MPa) | $b$ |
| Tool A | 273 ± 38 | 0.05 ± 0.03 | 141 ± 2.6 | 0.03 ± 0.01 | 1.0 ± 0.22 | 0.97 ± 0.08 |
| Tool B | 7 ± 0.01 | 0.21 ± 0.16 | 4.0 ± 0.37 | 0.43 ± 0.21 | 0.3 ± 0.00 | 1.00 ± 0.16 |
| Tool C | 11 ± 1.7 | 0.33 ± 0.18 | 0.2 ± 0.02 | 0.62 ± 0.13 | 1.0 ± 0.10 | 0.74 ± 0.16 |
| Tool D | 26 ± 1.7 | 0.12 ± 0.07 | 0.4 ± 0.02 | 0.55 ± 0.01 | 0.7 ± 0.00 | 0.81 ± 0.04 |
| Tool E | 19 ± 0.76 | 0.10 ± 0.08 | 4.0 ± 0.13 | 0.26 ± 0.07 | 0.4 ± 0.00 | 0.90 ± 0.14 |

the five cutting tools are also listed in Table IV. For a critical displacement of 1.0 mm, the average ratio of $\tau_a$ to the ultimate shear strength of the cement/bone interface was 0.24.

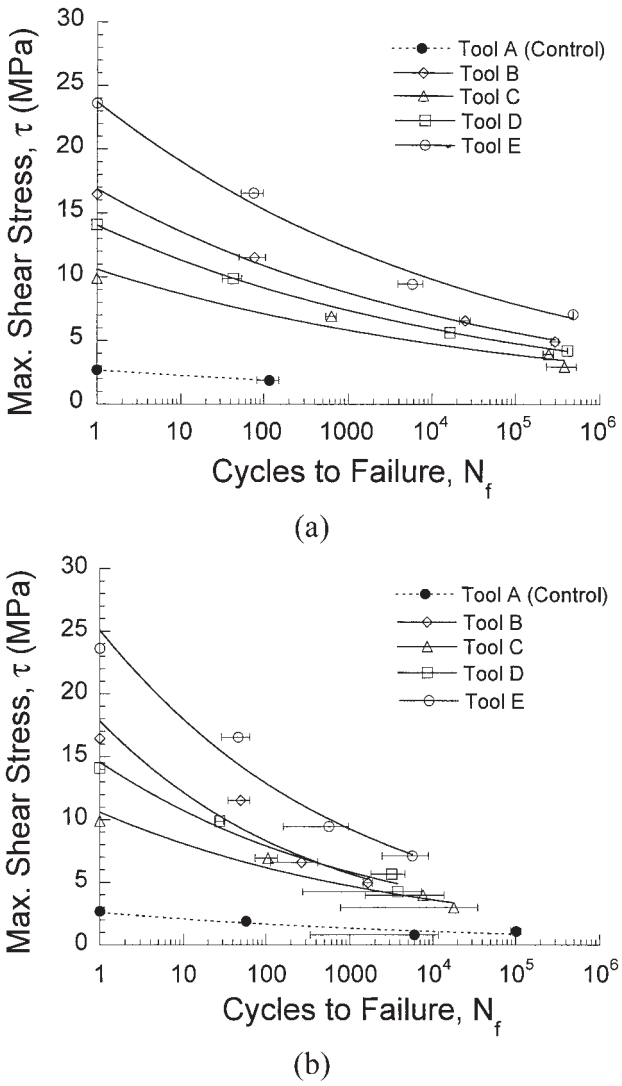


**Figure 7.** Stress life ($\tau$-$N$) diagrams for the model implants with failure defined in terms of a critical displacement describing the extent of loosening. (a) Failure defined by absolute displacement of the cement/bone interface of 1 mm, (b) failure defined by absolute displacement of the cement/bone interface to reach 0.20 mm.

## DISCUSSION

Push-out tests have served as the most common method for evaluating properties of the cement/prosthesis and cement/bone interfaces. In the present study, push-out tests were performed with model implants to evaluate properties of the cement/bone interface. Failure of all the specimens occurred through fracture of the cement/bone interface and the shear strength ranged from approximately 2–25 MPa. These results fall well within the range reported in previous investigations.[11–14] When evaluated in terms of the bone surface topography, the shear strength increased proportional to increases in $R_a$ and $V_i$ as shown in Figure 5(a,b), respectively. The ratio of shear strength resulting from the model implants prepared with the roughest surface (Tool E) and control surface (Tool A) was a factor of 10. Heiple et al.[40] found a similar trend in shear strength of the cement bone interface after the bone was roughened to enhance interdigitation. According to these results the shear strength of the cement/bone interface can be improved through an increase in bone surface roughness and volume of cement interdigitation. These qualities of the femoral canal are undoubtedly a function of the tools and procedures used in shaping the bone during surgical preparation.

Although the incidence and progression of loosening in cemented joint replacements is poorly understood, it is generally accepted that cyclic loads contribute to failure of the cement/bone interface. Loosening of the model implants was interpreted in terms of the absolute displacement ($\delta_{abs}$) of the stem with cyclic loading and in terms of the stress-life ($\tau$-$N$) response. In general, the $\delta_{abs}$ history exhibited three characteristic regions of response, as highlighted in Figure 4(a). These three regions are clearly evident from the responses of specimens prepared with the use of Tool E in Figure 6(a,b). Kim et al.[30,31] recently reported that the creep strain resulting from both cyclic tension and cyclic shear of the bone/cement interface followed a similar three-phase response. Also, clinical reports of loosening in cemented THRs have reported an initial period (post op. $<$ 6 months) characterized by rapid migration, followed by a reduction in rate of subsidence and development of a steady-state rate of displacement.[41,42] These periods are expected to be Regions I and II identified from the displacement history of the model joint replacements. Therefore, loosening in the model implants subjected

**TABLE IV. The Stress Life ($\tau$-$N$) Response for the Model Implants and the Apparent Fatigue Strength ($\tau_a$) Estimated from the Power Law Models for 1 and 10 Million Cycles to Failure**

| | $\delta_{abs}$ = 0.2 mm | | | | |
|---|---|---|---|---|---|
| Surface (Tool) | $\alpha$ (MPa) | $\beta$ | $R^2$ | $\tau_a$ (MPa) ($N_f = 10\times10^6$) | $\tau_a/\tau_{ult}$ |
| Tool A | 2.60 | −0.095 | 0.96 | 0.56 | 0.21 |
| Tool B | 17.85 | −0.166 | 0.96 | 1.23 | 0.08 |
| Tool C | 10.61 | −0.118 | 0.98 | 1.58 | 0.16 |
| Tool D | 14.59 | −0.133 | 0.99 | 1.71 | 0.12 |
| Tool E | 25.10 | −0.144 | 0.98 | 2.46 | 0.10 |
| | | | | | Avg. = 0.13 |
| | $\delta_{abs}$ = 1.0 mm | | | | |
| Surface (Tool) | $\alpha$ (MPa) | $\beta$ | $R^2$ | $\tau_a$ (MPa) ($N_f = 10\times10^6$) | $\tau_a/\tau_{ult}$ |
| Tool A | 2.69 | −0.075 | N/A | 0.80 | 0.30 |
| Tool B | 16.87 | −0.095 | 0.99 | 3.65 | 0.22 |
| Tool C | 10.60 | −0.087 | 0.95 | 2.61 | 0.26 |
| Tool D | 14.05 | −0.093 | 0.99 | 3.14 | 0.22 |
| Tool E | 23.73 | −0.096 | 0.99 | 5.09 | 0.22 |
| | | | | | Avg. = 0.24 |

to cyclic loads equivalent to 30% and 40% $\tau_{ult}$ appeared to be consistent with clinical observations of loosening and suggests that the primary mechanisms contributing to fatigue in both environments were similar. However, the monotonic increase in $\delta_{abs}$ (and short life) for specimens loaded at 70% $\tau_{ult}$ suggests that the results of these specimens were unique and the corresponding mechanisms of fatigue failure were quite different than those *in vivo*.

The apparent fatigue strength of the cement/bone interface ranged from approximately 0.5 to over 5 MPa, and was dependent on the critical displacement defining failure. A displacement of 1 mm over $10 \times 10^6$ cycles represents an average displacement of 0.1 mm/year. This measure is quite consistent with the rate of stem movement reported for patients with well-functioning THRs of 0.09 mm/year.[41] According to a numerical study of stresses in an anatomical models for a cemented THR, the maximum shear stress at the cement/bone interface is near 2 MPa.[43] Thus, experimental results in Table IV suggest that the cement/bone interface of the specimens prepared with Tool A would fail by fatigue. Fatigue failure of the interface would not likely cause total joint failure. However, the process would result in development of larger compressive normal stresses across the interface due to the degradation in mechanical interlock and an increase in subsidence. As expected from the large $\tau_{ult}$, specimens prepared with Tool E had the highest apparent fatigue strength. With the use of results of both monotonic and cyclic loading, the apparent fatigue strength of the interfaces is plotted in terms of the ultimate shear strength in Figure 8. Results are presented for two measures of critical displacement (0.2 and 1.0 mm) and life of $10 \times 10^6$ cycles. In general, the fatigue strength increased proportional to the ultimate shear strength. The strong correlation between $\tau_a$ and $\tau_{ult}$ for critical displacement of 1.0 mm (Figure 8; $R^2 = 0.99$) suggests that the $\tau_{ult}$ determined from push-out tests could be used to estimate the fatigue strength of the cement/bone interface. The aforementioned statement pertains to the mechanics contributing to loosening only and does not account for the biological factors that likely also contribute to the loosening process. It is important to note that the correlation between $\tau_a$ and $\tau_{ult}$ was not as strong for $\delta_{abs}$ of 0.2 mm ($R^2 = 0.77$). Interestingly, Walker et al.[44] reported from an evalu-

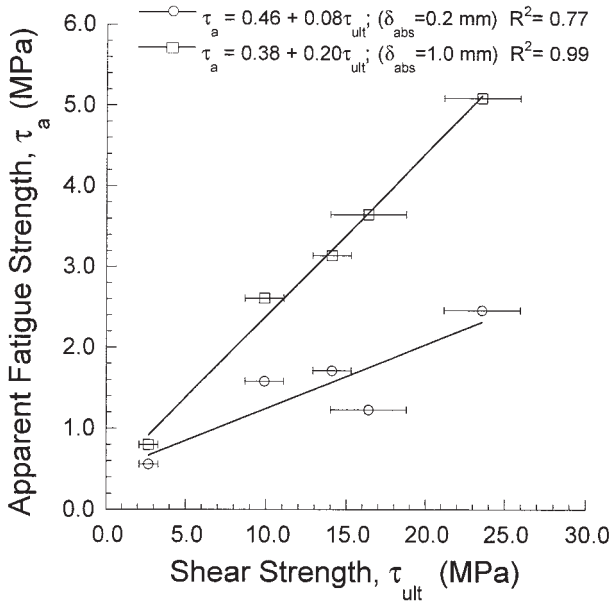


**Figure 8.** Relationship between the ultimate shear strength from push-out tests and the fatigue strength of the model implants (for $N_f = 10 \times 10^6$).

ation of successful cemented THRs using a radiograph analysis that a stem migration of less than 2 mm after 2 years was a forecast for long-term success. Thus, the use of a critical displacement of 0.2 mm is likely far too conservative.

The relationship between $R_a$, $V_i$, and the apparent fatigue strength of the cement/bone interface was examined with the use of results of the power-law models constructed from the $\tau$-$N$ responses in Figure 7. The fatigue strength (corresponding to $10 \times 10^6$ cycles) is plotted in terms of the $R_a$ of the bone in Figure 9(a). Similarly, the relationship between $V_i$ and the fatigue strength is shown in Figure 9(b). Interestingly, there appears to be a linear trend between the fatigue strength and both $R_a$ and $V_i$. These findings suggest that the fatigue strength of the cement/bone interface increases proportional to $R_a$ and $V_i$. Nevertheless, the evaluation was conducted with fatigue properties predicted with the use of models that were developed from results of relatively short-term experiments ($N \leq 500{,}000$ cycles). Future studies on the fatigue properties of the cement/bone interface and the influence of bone surface texture should be conducted and focus on the high-cycle fatigue response that arises with prolonged clinical use (10 years $<$ life). Furthermore, there is some deviation from the linear relationship between fatigue strength and $R_a$ and $V_i$, particularly for the model implants prepared with Tool B. The use of $R_a$ and $V_i$ for predicting the interface fatigue strength ignores the difference in fatigue strength between bone and cement. Also, neither parameter quantifies the potential challenge to interdigitation of cement within spatial features of the bone according to the profile shape. There appear to be other aspects of the bone profile height distribution that contribute to the fatigue response and have not yet been identified. Although the surface topography of bone necessary for optimizing the cement/bone interface remains unknown, the fatigue strength increases with the roughness and volume available for cement interdigitation.

Early migration of the prosthesis (within 500,000 cycles) has served as an indirect measure of performance in forecasting the long-term behavior. Kärrholm et al.[41] showed that a subsidence of 0.33 mm of a femoral hip component during the first postoperative 6 months is indicative of early loosening. Results of the fatigue experiments showed that the period of initial migration ($N_{IMA}$) corresponding to the Region I response was less than 60 kilocycles, which is equivalent to less than 1 month of postoperative function. The IMA was largest for specimens tested at 30% $\tau_{ult}$ (Table II). Because the magnitude of cyclic stress used for fatigue loading of the implants was not the same, the average IMA for each group of specimens in Table II was normalized by the maximum cyclic shear stress (IMA′). The apparent fatigue strength of the model implants ($\delta_{abs}$ of 1 mm) is plotted in terms of IMA′ in Figure 10. As evident in this figure, there is a strong correlation between the IMA′ and $\tau_a$ of the cement/bone interface. Thus, the IMA appears to be a function of both the surface topography and the magnitude of cyclic stress. A large IMA appears to be indicative of an interface with low fatigue strength. However, the reverse statement is not necessarily true. According to the trends in IMA with cyclic shear stress (Table II), a low IMA does not necessarily imply that the cemented device will exhibit a long fatigue life.

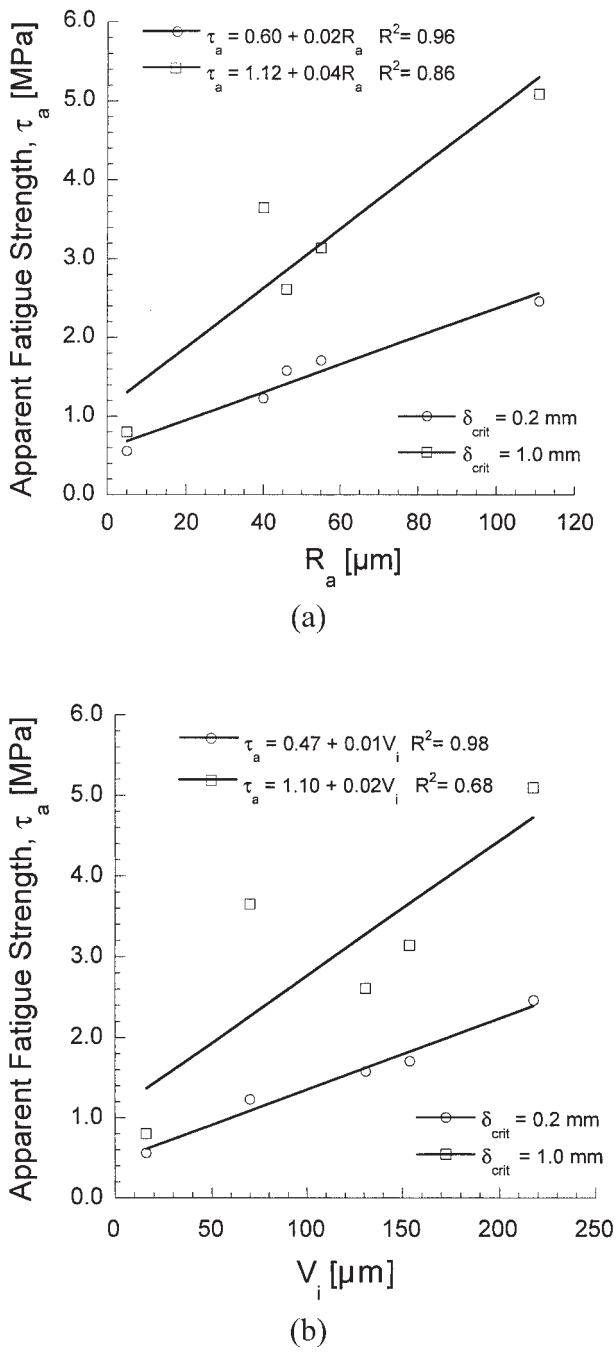


**Figure 9.** The influence of the surface topography of the femoral canal on the apparent fatigue strength of the cement/bone interface (for $N_f = 10 \times 10^6$). (a) Influence of average surface roughness ($R_a$), (b) influence of volume of interdigitation ($V_i$).

There are several limitations to the aforementioned experimental investigation and factors that potentially contributed to the fatigue strength of the cement/bone interfaces that warrant discussion. Loosening of the interface was examined in an environment comprised of mechanical factors only. Complications associated with the development of interface debris and development of fibrous tissue were not considered.

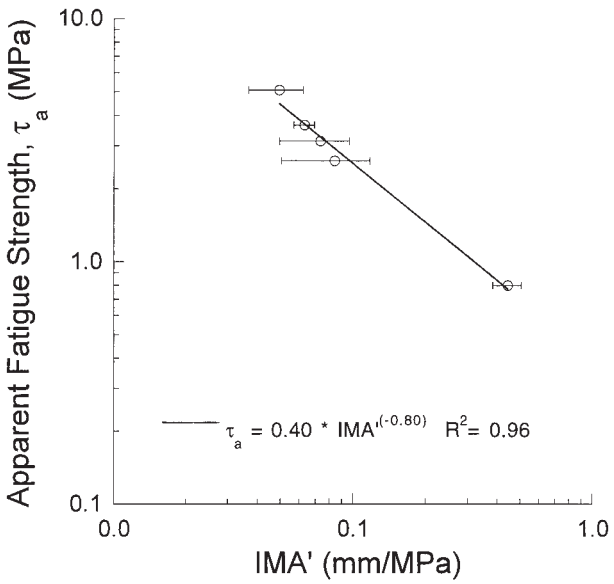


**Figure 10.** Relationship between the normalized initial migration amplitude (IMA′) and the apparent fatigue strength of the cement/bone interface. The IMA′ is the initial migration normalized by the maximum normal stress of the fatigue cycle. The IMA represented in this figure resulted from cyclic loading with a magnitude of 30% $\tau_{ult}$.

These factors would most likely elicit a synergistic response that potentially accelerates the loosening process with respect to results of the present study. Another recognized limitation of the study was the limited number of specimens prepared and examined. In the interest of examining a relatively wide range of surfaces, only three specimens were tested for each of the five surface preparations and stress ranges. Consequently, there are obvious limits to the statistical significance of the results. Cement pressure variations induced by the surface texture may have caused apparent differences in the fatigue strength. Also, the study examined interdigitation of cement and fatigue of the cement/bone interface with cortical bone, whereas interdigitation is more often achieved within trabecular bone. An evaluation focused on these concerns is under way. Nevertheless, this study has examined fatigue properties of the cement/bone interface and distinguished that the bone surface topography contributes to fatigue strength and potential for loosening. Surface preparations that increase the surface roughness and volume available for cement interdigitation can substantially increase the cement/bone interface fatigue strength. It appears that surgical tools may be used to texture the femoral canal which maximizes the interface fatigue strength.

## CONCLUSIONS

An experimental study of the influence from the bone surface texture on fatigue and loosening of the cement/bone interface in cemented joint replacements was conducted. Model hip replacements were prepared with the femoral canal textured with the use of specially designed cutting tools. Loosening was quantified as a function the stem migration resulting from cyclic loading. Based on the results from this study, the following conclusions were drawn.

- The average push-out strength of the model implant specimens ranged from 2.7 to 23.6 MPa and was dependent on the surface topography. The specimens with the largest average roughness ($R_a$) had the largest interfacial shear strength.
- The fatigue response of the model hip implants exhibited three characteristic regions of loosening beginning with an initial rapid growth in displacement (Region I), followed by a steady-state region (Region II), and ending in a rapid increase in displacement to failure (Region III). The presence of these three regions in the loosening response was dependent on the magnitude of cyclic loading and the bone surface topography.
- The apparent fatigue strength of the cement/bone interface was defined in terms of the cyclic shear stress required for a critical displacement (indicative of failure or loosening) within $10 \times 10^6$ cycles. For a critical displacement of 1 mm, the apparent fatigue strength ranged from 0.8 to 5.1 MPa. The ratio of the apparent fatigue strength to the ultimate shear strength of the interfaces ranged from 0.22 to 0.3, with an average of approximately 0.24.
- In general, the apparent fatigue strength increased proportional to the increase in $R_a$ of the femoral canal and the corresponding volume available for cement interdigitation ($V_i$).
- The apparent fatigue strength of the model implants was found to be strongly correlated with the normalized initial migration amplitude (IMA′). The model implants that exhibited the largest IMA′ also exhibited the lowest apparent fatigue strength.

## REFERENCES

1. Meek RM, Michos J, Grigoris P, Hamblen DL. Mid-term results and migration behaviour of a Ti-alloy cemented stem. Int Orthop 2002;26:356–360.
2. Jergesen HE, Karlen JW. Clinical outcome in total hip arthroplasty using a cemented titanium femoral prosthesis. J Arthroplasty 2002;17:592–599.
3. Bauer TW, Schils J. The pathology of total joint arthroplasty. II. Mechanisms of implant failure. Skeletal Radiol 1999;28:483–497.
4. Katz RP, Callaghan JJ, Sullivan PM, Johnston RC. Long-term results of revision total hip arthroplasty with improved cementing technique. J Bone Joint Surg 1997;79B:322–326.
5. Kavanagh BF, Ilstrup DM, Fitzgerald RH. Revision total hip arthroplasty. J Bone Joint Surg 1985;67A:517–526.
6. Berry DJ. Cemented femoral stems: what matters most. J Arthroplasty 2004;19:83–84.
7. Gardiner RC, Hozack WJ. Failure of the cement–bone interface. A consequence of strengthening the cement–prosthesis interface? J Bone Joint Surg 1994;76B:49–52.
8. Mohler CG, Callaghan JJ, Collis DK, Johnston RC. Early loosening of the femoral component at the cement–prosthesis interface after total hip replacement. J Bone Joint Surg 1995;77A:1315–1322.

9. Mann KA, Bartel DL, Wright TM. The effect of using a plasma-sprayed stem-cement interface on stresses in a cemented femoral hip component. Trans Orthop Res Soc 1992;38:317.
10. Ramaniraka NA, Rakotomana LR, Leyvraz PF. Effects of stem stiffness, cement thickness, and roughness of the cement–bone surface. J Bone Joint Surg 2000;82B:297–303.
11. Halawa M, Lee AJ, Ling RS, Vangala SS. The shear strength of trabecular bone from the femur, and some factors affecting the shear strength of the cement–bone interface. Arch Orthop Trauma Surg 1978;92:19–30.
12. Moran JM, Greenwald AS, Matejczyk MB. Effect of gentamicin on the shear and interface strength of bone cement. Clin Orthop 1978;141:96–101.
13. Rosenstein A, MacDonald W, Iliadis A, McLardy-Smith P. Revision of cemented fixation and cemented-bone interface strength. Proc Inst Mech Eng H 1992;206:47–49.
14. Wang X, Subramanian A, Dhanda R, Agrawal M. Testing of bone–biomaterial interfacial bonding strength; a comparison of different techniques. J Bone Joint Surg 1997;79B:181–182.
15. Askew MJ, Steege JW, Lewis JL, Ranieri JR, Wixson RL. Effect of cement pressure and bone strength on polymethylmethacrylate fixation. J Orthop Res 1984;1:412–420.
16. Krause WR, Krug W, Miller J. Strength of the cement–bone interface. Clin Orthop 1982;163:290–299.
17. Majkowski RS, Bannister GC, and Miles AW. The effect of bleeding on the cement-bone interface. Clin. Orthop. 1994;299: 293-297.
18. Majkowski RS, Miles AW, Bannister GC, Perkins J, Taylor JS. Bone surface preparation in cemented joint replacement. J Bone Joint Surg 1993;75B:459–463.
19. Mann KA, Ayers DC, Werner FW, Nicoletta RJ, Fortino MD. Tensile strength of the cement–bone interface depends on the amount of bone interdigitated with PMMA cement. J Biomech 1997;30:339–346.
20. Crowninshield RD, Jennings JD, Laurent ML, Maloney WJ. Cemented femoral component surface finish mechanics. Clin Orthop 1998;355:90–102.
21. Huiskes R, Verdonschot N, Nivbrant, B. Migration, stem shape, and surface finish in cemented total hip arthroplasty. Clin Orthop 1998;355:103–112.
22. Mann KA, Werner FW, Ayers DC. Mechanical strength of the cement–bone interface is greater in shear than in tension. J Biomech 1999;32:1251–1254.
23. Verdonschot N, Huiskes R. Mechanical effects of stem cement interface characteristics in total hip replacement. Clin Orthop 1996;329:326–336.
24. Bean DJ, Convery FR, Woo SLY, Lieber RL. Regional variations in shear strength of the bone–polymethylmethacrylate interface. J. Arthroplasty 1987;2:293–398.
25. Choi K, Goldstein, SA. A comparison of the fatigue behavior of human trabecular and cortical bone tissue. J Biomech 1992;25: 1371–1381.
26. Taylor M, Tanner KE. Fatigue failure of cancellous bone: A possible cause of implant migration and loosening. J Bone Joint Surg 1997;79B:181–182.
27. Krause WR, Mathis RS. Fatigue properties of acrylic bone cements: Review of the literature. J. Biomed. Mater Res Appl Biomater 1988;22:338–347.
28. Lu X, Topoleski LD. A controlled-notch specimen to study fatigue crack initiation in bone cement. J Biomed Mater Res 2000;53:505–510.
29. Lewis G, Janna SI. Effect of fabrication pressure on the fatigue performance of Cemex XL acrylic bone cement. Biomaterials 2004;25:1415–1420.
30. Kim DG, Miller MA, Mann KA. A fatigue damage model for the cement–bone interface. J Biomech. 2004;37:1505–1512.
31. Kim DG, Miller MA, Mann KA. Creep dominates tensile fatigue damage of the cement–bone interface. J Orthop Res 2004;22:633–640.
32. Gustafson MB, Martin GW, Gibson V, Storms DH, Stover SM, Gibeling J, Griffin L. Calcium buffering to maintain bone stiffness in saline solution. J. Biomech 1996;29:1191–1194.
33. Arola DD, Yang DT, Stoffel KA. The apparent volume of interdigitation: A new parameter for evaluating the influence of surface topography on mechanical interlock. J Biomed Mater Res Appl Biomater 2001;58:519–524.
34. Arola D, Stoffel KA, Yang DT. Fatigue of the cement/bone interface: Surface texture and wear debris. Submitted for publication.
35. Fisher DA, Tsang AC, Paydar N, Milionis S, Turner CH. Cement-mantle thickness affects cement strains in total hip replacement. J Biomech 1997;30:1173–1177.
36. Davies JP, Harris WH. *In vitro* and *in vivo* studies of pressurization of femoral cement in total hip arthroplasty. J Arthroplasty 1993;8:585–591.
37. Davy DT, Kotzar GM, Brown RH, Heiple KG, Goldberg VM, Heiple Jr. KG, Berilla J, Burnstein AH. Telemetric force measurements across the hip after total hip arthroplasty. J Bone Joint Surg 1988;70A:45–50.
38. Bergmann G, Deuretzbacher G, Heller M, Graichen F, Rohlmann A, Strauss J, Duda GN. Hip contact forces and gait patterns from routine activities. J Biomech 2001;34:859–871.
39. Morlock M, Schneider E, Bluhm A, Vollmer M, Bergmann G, Muller V, Honl M. Duration and frequency of every day activities in total hip patients. J Biomech 2001;34:873–881.
40. Heiple KG, Shea KL, Nelson DL, Davy DT. Enhancement of the shear strength of the bone-methacrylate interface. Transactions of the 32nd Orthop. Res. Soc. Meeting; 1986. p 354.
41. Kärrholm J, Borssen B, Lowenhielm G, Snorrason F. Does early micromotion of femoral stem prosthesis matter? J Bone Joint Surg 1994;76B:912–917.
42. Alfaro-Adrian J, Gill HS, Murray DW. Cement migration after THR. A comparison of Charnley Elite and Exeter femoral stems using RSA. J Bone Joint Surg 1999;81B:130–134.
43. Brown TD, Pedersen DR, Radin EL, Rose RM. Global mechanical consequence of reduced cement/bone coupling rigidity in proximal femoral arthroplasty: A three-dimensional finite element analysis. J Biomech 1988;21:115–129.
44. Walker P, Mai SF, Cobb AG, Bentley G, Hau J. Prediction of clinical outcome of THR from migration measurements on standard radiographs. J Bone Joint Surg 1995;77B:705–714.